Technical Report
UKY 31-70-MET 13

K

RESEARCH STUDY OF DAMAGE PRODUCED IN SILICON SEMICONDUCTORS BY NEUTRON IRRADIATION

Final Report

by

GORDON A. SARGENT
Department of Metallurgical Engineering
and Materials Science

OFFICE OF RESEARCH AND ENGINEERING SERVICES
COLLEGE OF ENGINEERING
UNIVERSITY OF KENTUCKY

COLLEGE OF ENGINEERING
UNIVERSITY OF KENTUCKY

ADMINISTRATIVE ORGANIZATION

Robert M. Drake, Jr., Ph.D.
Dean, College of Engineering and
Director, Office of Research and Engineering Services

David K. Blythe, M.C.E.
Associate Dean, Continuing Education and Extension,
College of Engineering

James E. Funk, Ph.D.
Associate Dean, Graduate Programs, College of Engineering

Warren W. Walton, M.S.
Assistant Dean, College of Engineering

Blaine F. Parker, Ph.D.
Chairman, Department of Agricultural Engineering

Robert B. Grieves, Ph.D.
Chairman, Department of Chemical Engineering

Staley F. Adams, Ph.D.
Chairman, Department of Civil Engineering

Robert L. Cosgriff, Ph.D.
Chairman, Department of Electrical Engineering

Oscar W. Dillon, D.Eng.Sci.
Chairman, Department of Engineering Mechanics

Roger Eichhorn, Ph.D.
Chairman, Department of Mechanical Engineering

Hans Conrad, D.Eng.
Chairman, Department of Metallurgical Engineering

Russell E. Puckett, M.S.
Associate Director, Office of Research and
Engineering Services

Technical Report UKY 31-70-MET 13

RESEARCH STUDY OF STRUCTURAL DAMAGE PRODUCED IN SILICON SEMICONDUCTORS BY NEUTRON IRRADIATION

Final Report

by

GORDON A. SARGENT
Department of Metallurgical Engineering
and Materials Science

June 1969 to July 1970

This work was performed for the Jet Propulsion Laboratory, California Institute of Technology (Contract 952561), as sponsored by the National Aeronautics and Space Administration under Contract NAS 7-100.

ABSTRACT

The main objectives of this program are to attempt to determine the size distribution, morphology, and structural characteristics of the regions of lattice disorder which are produced by bombarding undoped and lithium doped silicon solar cells, produced from both float zone melted and crucible pulled material, with neutrons.

The research has been carried out entirely on the electron microscope using the techniques of surface replication, electron transmission, and electron diffraction.

Evidence for the presence of precipitated metallic lithium was found in all the doped float zone melted samples and there was some indication of an oxide precipitate in the pulled samples.

Crater defects which were thought to be associated with the space charge region around vacancy clusters were observed in all of the samples of the irradiated float zone material. Similar defects were only observed in the most heavily doped and irradiated crucible pulled material. It was concluded that the presence of oxygen in the pulled material may be an efficient trap which prevents the formation of the large defect clusters.

The crater defect density was found to increase with increasing irradiation dose and increasing lithium content, however, the defect size was found to decrease with increasing dose and increasing lithium.

The crater defects were found to be stable at temperatures between 300° and 900°K. Significant annealing was found only in the undoped samples which were irradiated at the lowest doses. In the pulled material, no annealing was found until a temperature of 1200°K was reached.

TABLE OF CONTENTS

1. INTRODUCTION

1.1. Research Program

The purpose of this research program was to determine the effects of neutron irradiation on the structural characteristics of undoped and lithium doped silicon solar cells. The main objectives of the program were to attempt to determine the size, distribution, morphology and general structural characteristics of the regions of lattice disorder produced in P/N silicon solar cells by bombardment with mono-energetic neutrons having energies of about 14.7 MeV.

The occurrence of the damage produced by the neutron bombardment was studied as a function of a number of experimental variables, including method of silicon crystal growth, lithium doping level, and the irradiation dose. Also, annealing experiments were carried out on the samples after irradiation to determine whether or not there was any change in morphology or distribution of the defects with increased temperature.

The experimental investigation was carried out entirely by electron microscopy. Two main experimental techniques were used: (1) surface replication, and (2) thin-film transmission electron microscopy. Additional studies were carried out on the thin-film samples using the technique of selected area electron diffraction analysis.

The samples were irradiated with mono-energetic neutrons in a Cockroft-Walton neutron generator.

1.2. Literature Survey

It is now generally accepted that a localized cluster of lattice defects may be produced by a recoil from a single collison between an energetic neutron and an atom in the lattice (1-5). The recoil is thought to produce the cluster of defects when its energy is below the threshold required to produce ionization. The energy of the recoil is dissipated by creating lattice disorder (or generating a "thermal spike"). Rapid quenching of

the "spike" should freeze a large concentration of lattice defects in the neighborhood.

In certain cases the characteristics of the disordered regions might differ quite strikingly from the surrounding undisturbed material. For example, the asymptotic state of irradiated germanium is p-type, while the asymtotic state of irradiated silicon is compensated intrinsic. Hence, disordered regions in n-type germanium should be p-type, while those in extrinsic silicon should be intrinsic. If this is the case then, one could expect that the disordered regions would be surrounded by potential wells of sufficient depth as to noticeably influence the bulk electrical properties of the material. Until recently, the behavior of irradiated semiconductors has been interpreted on the basis of isolated Frenkel defects in terms of the model by James and Lark-Horovitz, (6). However, Gossick (7) and Crawford and Cleland (8) have proposed a model of disordered regions more applicable to neutron irradiated semiconductors which predicts the existence of regions of highly localized damage. Their model for a hypothetical region of lattice disorder is described as follows. In extrinsic p-type silicon the region of disorder is considered to be intrinsic. Although in reality the actual shape of the region may be irregular, it is assumed to be spherical. The concentration of defects is considered to change abruptly at the boundary between the disturbed region and the undisturbed matrix. Surrounding a disordered region is a potential well, which arises because the position of the Fermi level relative to the energy bands is different within the disordered region compared to the outside. Crawford and Cleland have suggested that a disordered region would contain from 10^5 to 10^6 atoms, which distributed in a spherical region, would give a radius of 150 to 200 Å. Beyond the radius of the disturbed region, a space charge-region (junction) is created, the dimensions of which would depend upon the carrier concentration of the unirradiated material. For p-type silicon this is predicted to be of the order of 2000 to 2500 Å in diameter.

Subsequently, experimental measurements of electrical properties by Closser (9) and Stein (10) have provided direct evidence for the existence of the damaged regions as predicted by the theoretical models of Gossick and Crawford and Cleland. In the above experiments the decrease in electrical conductivity of silicon was used as a measure of the carrier removal as a result of neutron irradiation, and the carrier concentration was obtained from Hall coefficient measurements. Further electrical property studies by Stein (11) have shown that neutron irradiation at 76°K produces light sensitive defects at a rate that is independent of the concentration of crystal impurities. It was concluded that these defects, which were produced in n-type silicon, were vacancy-liberating clusters. The neutron induced defects were thus regarded as regions of high resistivity surrounded by a space-charge region. Such a combination of defects and space-charge regions could be regarded as insulators in an otherwise conducting medium. The light sensitivity of the electrical conductivity of the irradiated silicon is believed to result from minority carrier trapping, within the cluster-space-charge regions, which effectively reduces the insulating volume. More recently, Stein (12) has shown that the behavior of defects produced in p-type silicon by neutron irradiation at 76°K was independent of the method of crystal growth. He also found that annealing the samples produced several diffuse stages of recovery between 150 and 550°K, with the largest stage between 150 and 240°K.

To date very little work has been carried out to determine the exact structural nature of the regions of lattice disorder created by irradiation. Fujita and Gonser (13) have attempted to determine the size of the damaged regions in irradiated germanium using an X-ray diffraction technique, but this technique did not provide any useful information about the distribution or morphology of the defects present. More recently, however, there have been several attempts to observe the damaged regions in neutron irradiated germanium and silicon semiconductors more directly using the technique of electron microscopy.

The first direct observation of defect clusters was made by Parsons, Balluffi and Koehler (14) in thin films of germanium using transmission electron microscopy. The number of defect regions which they observed was in good agreement with their theoretical estimates from electrical property measurements and a mean defect diameter of 53 Å was measured. Hemment and Gunnersen (15) have attempted to perform similar transmission electron microscopy on n-type silicon samples which were irradiated with fast neutrons with integrated doses ranging from 5×10^{16} to 10^{19} neutrons/cm^2 but they were unable to observe any defects. Their inability to resolve defects may have been due to the difficulty which they experienced in preparing good thin foils for their transmission work. More recently, however, Pankratz, Sprague and Rudee (16) have successfully observed defect clusters in neutron irradiated silicon by transmission electron microscopy. They found that the mean defect image size was dependent on the impurity content and on the annealing treatment, ranging from a maximum of about 40 Å in the as irradiated material to 22 Å in the annealed material. Also it was found that the defect density was proportional to the irradiation dose.

An alternative method for observing defects in germanium and silicon semiconductors, which was tried unsuccessfully by Chang (17) and Noggle and Stiegler (18), and later perfected by Bertolotti and his co-workers (19, 20,21,22) consists of irradiating the semiconductor with fast neutrons, etching with suitable chemicals and then constructing a replica of the surface for observation in the electron microscope.

Bertolotti and his co-workers have irradiated silicon samples with 14 MeV neutrons produced by a Van de Graaff accelerator to a fluence of 6×10^{12}/cm^2. They found that upon etching the surface of the irradiated samples craters were produced, the dimensions of which were found to compare with the dimensions of the space-charge regions as calculated according to the theory of Gossick (7) and Crawford and Cleland (8). Within the craters a small well defined region could also

be observed which compared favorably with the theoretical estimates for the size of the damaged region in the lattice.

The observations by Bertolotti et al. seem to agree well with the picture proposed by Gossick of the creation of highly localized defect clusters in neutron irradiated semiconductors, and with the existence of a junction or space-charge region between the defect cluster and the undamaged matrix.

The work undertaken in the present contract was designed to extend this earlier work specifically to try to determine the true structural nature of the damaged regions, to study the effects of annealing these regions, and to study the effects of lithium doping on them.

It was decided to use neutrons as the irradiating particles since (1) damage effects of charge are absent leading to possibly simpler interpretation of the data, (2) the momentum of the particle can be easily controlled by means of an available source, and (3) the momentum damage produced by neutrons should be directly comparable to that produced by protons of similar energies. Thus the work undertaken here was designed to contribute to the understanding and possible solution of the problem of damage caused to silicon solar cells by high momentum particles.

2. EXPERIMENTAL TECHNIQUE

2.1. Material

The experimental work described in this report was carried out entirely on commercial lithium doped silicon solar cells obtained from Heliotek, a division of Textron Incorporated. Cells were produced from two types of starting material: float zone refined single crystals of phosphorous doped n-type silicon cut to give (110) crystal slices, and pulled single crystals of n-type silicon cut to give (100) crystal slices. Boron was then diffused into the slice to give a junction depth of 0.5 micron. Lithium was then diffused in using the "paint on" technique, to produce four types of cells, according to the following schedule: (a) no lithium

diffusion, (b) 1 x 10^{15} lithium atoms/cm^3 - diffusion for 5 minutes and redistributed 120 minutes at 350°C, (c) 1 x 10^{16} lithium atoms/cm^3 - diffused 5 minutes and redistributed 60 minutes at 425°C, and (d) 1 x 10^{17} lithium atoms/cm^3 - diffused 90 minutes and redistributed 60 minutes at 425°C.

2.2 Neutron Irradiation

Samples of the undoped and lithium doped solar cells were irradiated with neutrons produced by a Cockroft-Walton generator, to doses of approximately 10^{10}, 10^{11}, 10^{12} and 10^{13} neutrons/cm^2. The neutrons were produced by bombarding a tritium target with deuterium gas molecules. This source of neutrons is highly mono -energetic and produces neutrons with energies of approximately 14.7 MeV. The samples were irradiated at room temperature, the dose being controlled by varying the distance of the sample from the target. The relative dose of each sample was measured by placing a thin copper foil of known weight behind each of the cells and after irradiation monitoring the decay of the Cu^{62} isotope, which has a half-life of 9.9 minutes.

After irradiation the samples were sectioned by means of a diamond saw for examination by surface replication and transmission electron microscopy.

2.3 Specimen Preparation for Surface Replication

The surface of the solar cells was prepared for replication by mechanically grinding and polishing and then by etching with CP4A etchant (15 cc acetic acid, 25 cc nitric acid, and 15 cc hydroflouric acid). A replica was then made of the etched surface by evaporating a thin layer of carbon onto it. To add mechanical strength to the carbon and to aid in its removal from the surface, an additional layer of chromium metal was deposited by evaporation. The replica was then removed from the surface by means of mylar tape which was subsequently removed by dissolving in acetone. The replica was then observed by transmission electron microscopy at an accelerating voltage of 75 KV.

2.4 Specimen Preparation for Thin Foil Electron Microscopy

Small samples of approximately 1 mm^2 in size were cut from the solar cells and chemically thinned to about 0.1 mm in a solution consisting of 9 parts nitric acid and 1 part hydroflouric acid. After chemical polishing the sample was placed in a plastic holder which had a small hole in the center, and the polishing was continued until a small dimple was produced in the surface of the sample. The outer edges of the sample were then painted with an enamel paint and the chemical polishing was resumed. The upper surface of the specimen was observed through a binocular microscope. A light source was used to illuminate the back side of the specimen and polishing was continued until yellow colored light could be observed through the specimen. At this stage the specimen was approximately 5000 Å thick. Additional polishing beyond this stage resulted in complete perforation and the thinned down section rapidly rounded off leaving the section too thick to be observed by transmission electron microscopy. After thinning to the yellow light stage, the specimen was washed using a sequence of cleaning agents (distilled water, acetone, distilled water, and finally methanol).

Initially some difficulty was experienced in observing the samples by transmission electron microscopy due to charge build-up on the surface of the specimen as soon as the electron beam hit it. It was found, however, that if the specimen was sandwiched between two copper grids then the charge could be adequately grounded and a much improved image was produced.

2.5 Thermal Annealing Experiments

In order to study the recovery of the neutron irradiation induced defect structure, samples were annealed at temperatures of 293°, 593°, 700°, 900° and 1200°K. After annealing the samples were examined by transmission electron microscopy and surface replication as described in Sections 2.3 and 2.4. For transmission electron microscopy two

annealing techniques were used. In the first technique the sample was prepared as a thin foil and annealed in the electron microscope using a hot stage specimen holder. In this method the specimen was heated by conduction from a small resistance heater wound around the specimen holder. In the second technique small samples of the solar cell (about 1 mm^2) were annealed in bulk form in a vacuum furnace (10^{-6} torr). An annealing time of 10 minutes at temperature was used for all experiments.

3. RESULTS AND DISCUSSION

3.1 The Float Zone Melted Solar Cell Material

3.1.1 Neutron Irradiation Damage and the Effect of Lithium Doping

A thin film electron transmission picture of the unirradiated solar cell material without lithium doping is shown in Figure 1 . There is no significant detail to be observed in this picture, except for the broad diffraction contour lines typical of a thin flat specimen without secondary structure. No dislocation lines are visible in this field of view. A selected area diffraction pattern taken of this field is shown in Figure 2(a). An interpretation of this diffraction pattern is shown in Figure 2(b). The pattern can be indexed as diamond cubic with a $[1\bar{1}0]$ zone axis.

Figure 3 shows an electron transmission picture obtained from a thin foil of the unirradiated solar cell material doped with 10^{17} lithium atoms per cm^3. The structure here appears to contain many small dark spots or precipitates distributed fairly homogeneously throughout the whole field of view. A selected area diffraction pattern taken from an area such as that in Figure 3 is shown in Figure 4(a). An interpretation of this diffraction pattern is given in Figure 4(b). A number of weaker diffraction spots can be observed which cannot be indexed with the diamond cubic structure of the silicon matrix. They can, however, be indexed as body-centered-cubic. By comparing the radius ratios of the selected area diffraction spots and assuming a value for the lattice parameter of the matrix, it was found that the lattice parameter of the body-centered cubic structure is approximately 3.45 Å. This value agrees well with that for

Figure 1. Transmission electron micrograph of an undoped unirradiated solar cell.

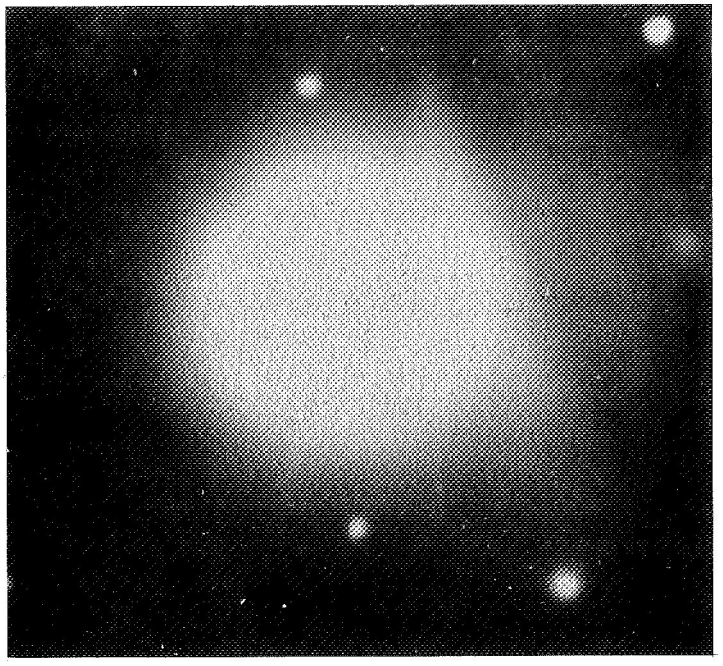

Figure 2(a). Electron diffraction pattern taken from an area similar to that shown in Figure 1.

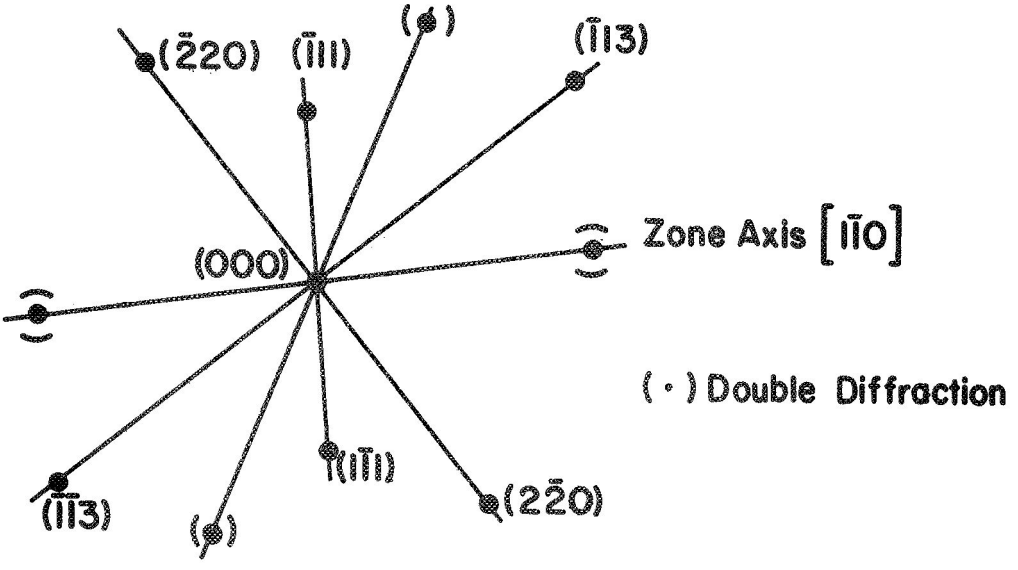

Figure 2(b). Interpretation of the diffraction pattern shown in Figure 2(a).

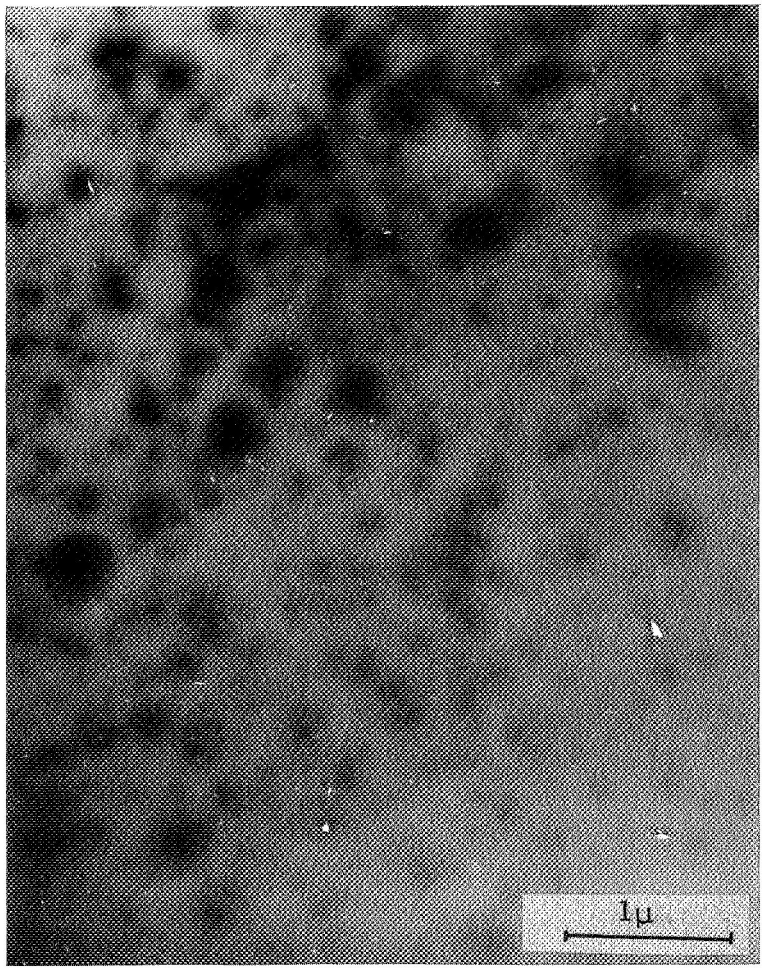

Figure 3. Transmission electron micrograph of an unirradiated solar cell which was doped with 10^{17} lithium atoms/cm^3.

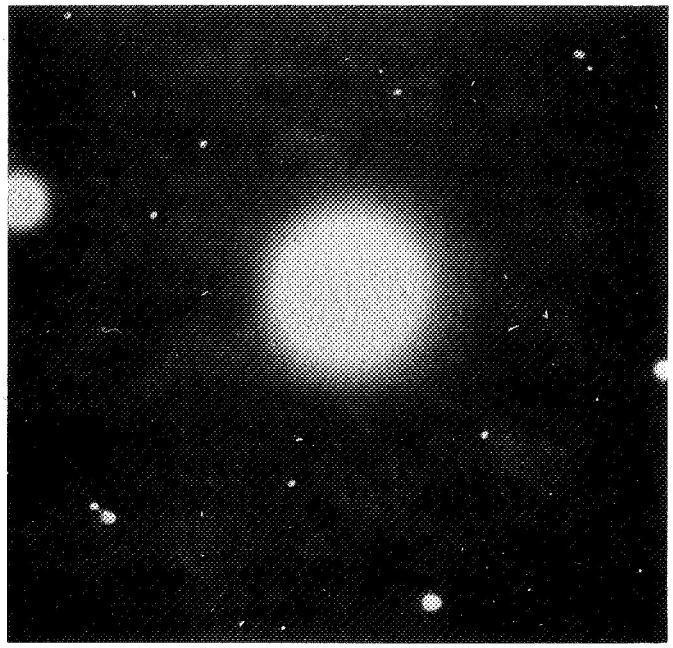

Figure 4(a). Electron diffraction pattern taken from an area such as that shown in Figure 3.

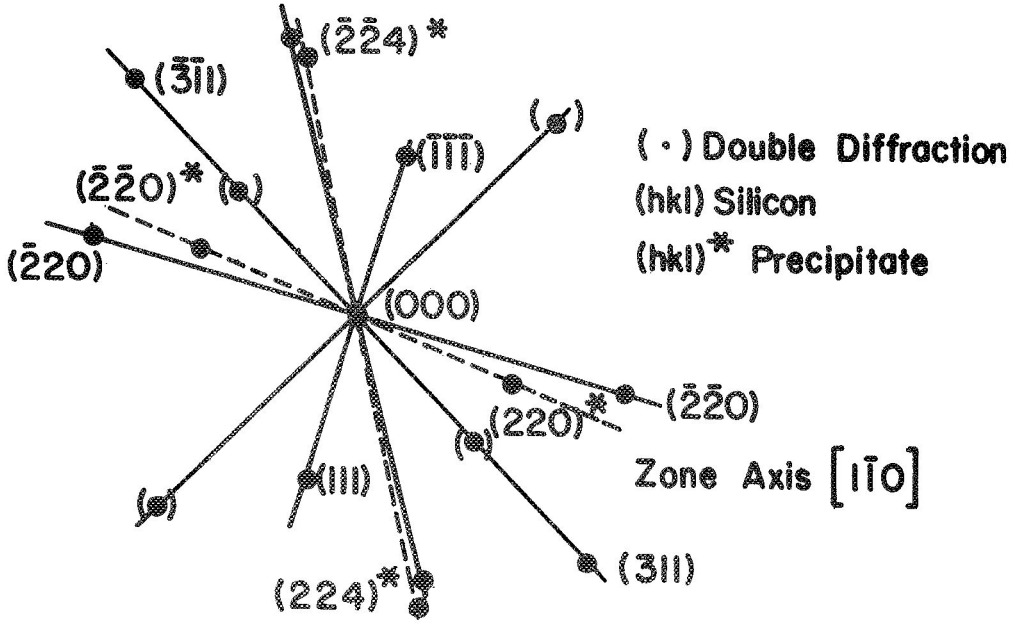

Figure 4(b). Interpretation of the diffraction pattern shown in Figure 4 (a).

the lattice parameter of lithium. It appears probable, therefore, that the dark spots observed in the lithium doped cells are due to excess lithium precipitated out of solution in the silicon matrix. It can be seen from Figure 4(b) that there appears to be some indication of an orientation relationship between the precipitate and the matrix. For example, the $(1\bar{1}0)$ planes of the precipitate particles are almost parallel (within about 5°) to the (110) planes of the matrix. The effective macroscopic cross-section for the electron diffraction was approximately five microns square. From such a diffraction pattern it is not possible to measure the density of the precipitates which give rise to the additional diffraction spots. Observations similar to those described above were observed in all of the lithium doped samples. It would appear, therefore, that the usual technique used to measure the lithium concentration, i.e. electrical resistivity measurements, is not particularly accurate when the solubility limit of the matrix is exceeded, as appears to have been the case with the present batch of samples.

Figure 5 shows a picture obtained in the electron microscope of a surface replica taken from the etched surface of an unirradiated sample which contained no lithium. This photograph shows a finely etched uniform structure without any significant features.

Figure 6 shows a surface replica from a sample which was undoped but irradiated with 10^{11} neutrons/cm^2. This photograph is a typical example of the appearance of the etched surfaces of the samples after neutron irradiation. The area shows a finely etched background structure on which many crater like depressions can be observed. Figure 7 shows a typical micrograph obtained from a replica of the lithium doped and irradiated material. Here, although the surface preparation was the same, the background structure is a little more irregular and numerous small pits can be observed, as well as the craters. The difference in the appearance of the doped and undoped material could be related to the presence of lithium which possibly modifies the etching characteristics slightly.

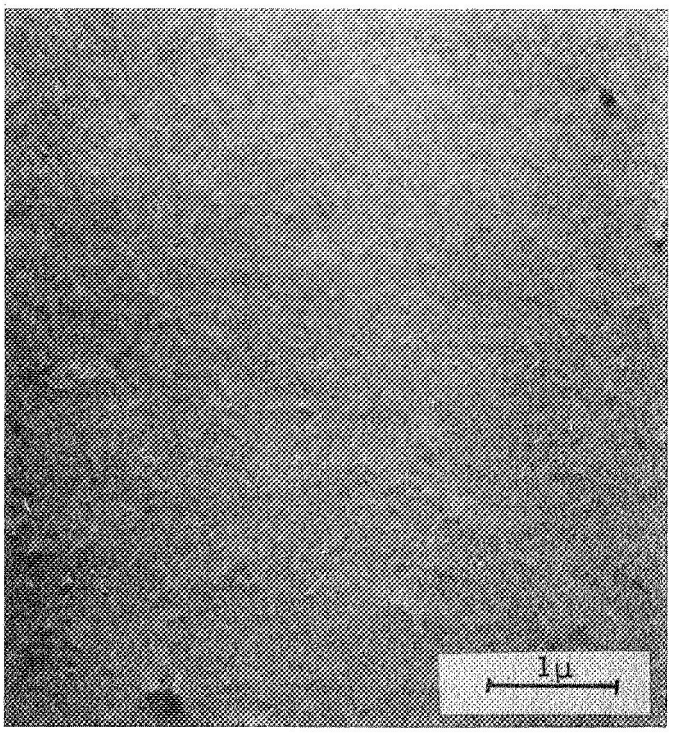

Figure 5. Surface replica of an undoped and unirradiated solar cell.

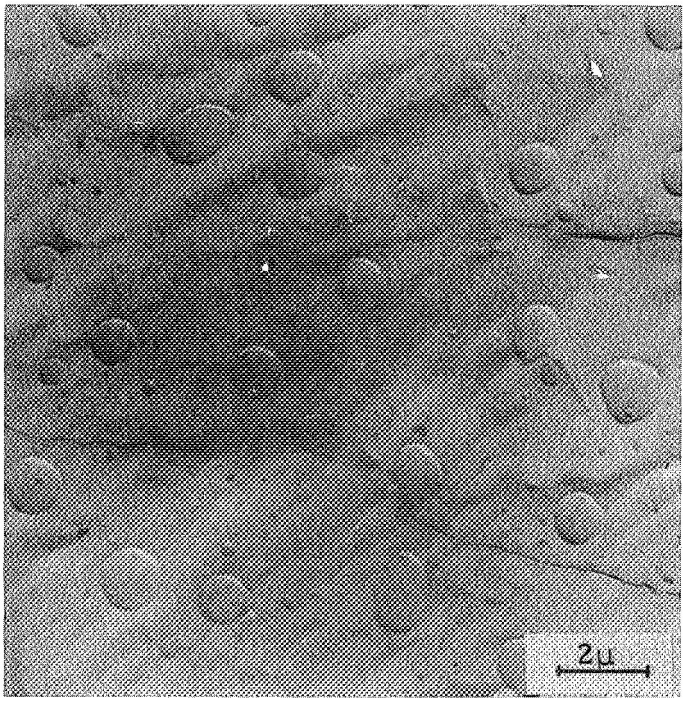

Figure 6. Surface replica of an undoped solar cell irradiated with 10^{11} neutrons/cm^2.

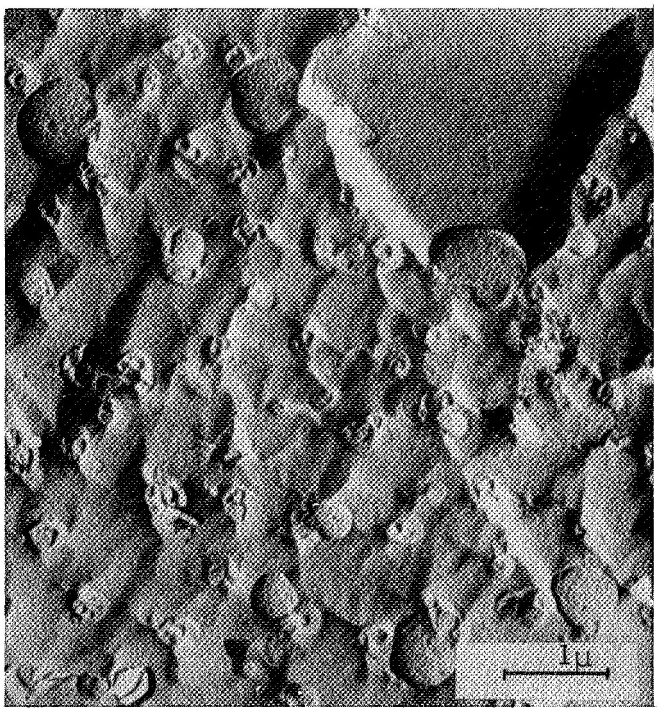

Figure 7. Surface replica of a solar cell doped with 10^{17} lithium atoms/cm^3 and irradiated with 10^{12} neutrons/cm^2.

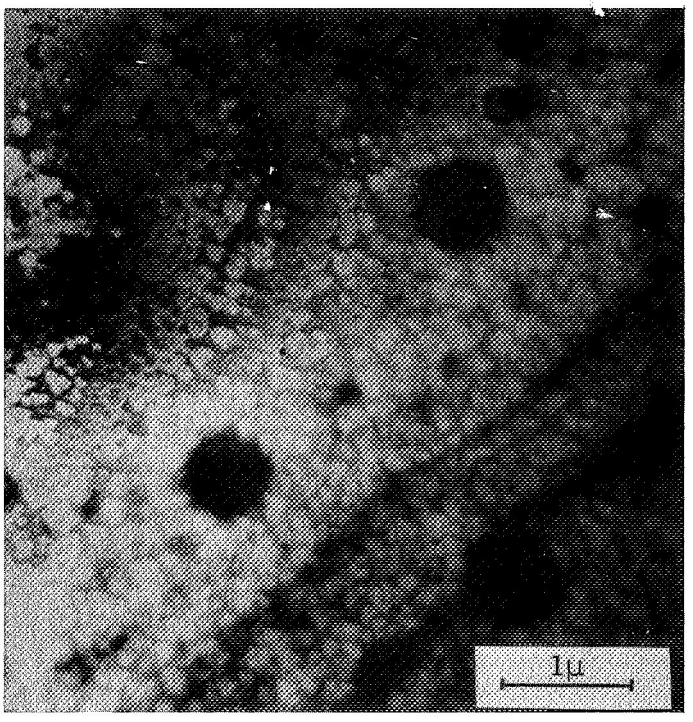

Figure 8. Electron transmission micrograph of an undoped solar cell irradiated with 10^{12} neutrons/cm^2.

Figure 8 shows an electron transmission picture obtained by chemically thinning a sample cut from one of the undoped cells which was irradiated to a dose of 10^{12} neutrons/cm^2. In this field of view the dark circular areas appear to correspond to the craters which are revealed by the surface replication technique. It is possible that these images are actually produced by cratering of the surface of the thin transmission specimen, which would then give rise to a difference in the thickness of the specimen in this region, and hence, produce a different electron intensity in transmission. It is not clear, at the present time, what the background structure represents. It appears to consist of triangular shaped images, and could possibly be due to stacking faults.

According to the Gossick theory, the dimensions of the craters revealed by the above techniques actually correspond to the size of the space-charge region which surrounds a cluster of lattice defects formed during the irradiation. Therefore the density of the craters should relate to the total number of defects produced at a particular irradiation dose.

The average density and diameter of the craters were measured as a function of the dose and amount of dopant. The average values were obtained from measurements made upon six different areas of replicated surface. These areas were chosen at random in the electron microscope. Generally it was observed that in the undoped material, as can be seen from Figure 6, the irradiation damage appeared to be uniformly distributed throughout the specimen. However, this was found to be less so in the lithium doped and irradiated material. This could possibly be associated with the distribution and presence of lithium precipitates in the doped specimens.

Values of the average density and diameter of the crater defects are presented in Table I for the various irradiation doses and doping concentrations. These results are presented graphically in Figures 9 and 10, respectively. The experimental error for the crater diameter measurements was approximately 5%. The spread of values about the

TABLE I.

Effect of Neutron Irradiation and Lithium Doping Level on Defect Density and Defect Size at 300°K

Lithium atoms/cm^3	Dose Φ n/cm^2	Average Defect density (#/cm^2)	Average Defect diameter (Å)
0	10^{10}	6.5×10^6	1.5×10^4
	10^{11}	1.0×10^7	1.2×10^4
	10^{12}	1.7×10^7	6.0×10^3
	10^{13}	5.4×10^7	3.3×10^3
10^{15}	10^{10}	1.0×10^7	8.3×10^3
	10^{11}	1.5×10^7	8.0×10^3
	10^{12}	2.0×10^7	5.0×10^3
	10^{13}	7.1×10^7	3.0×10^3
10^{16}	10^{10}	2.0×10^7	7.5×10^3
	10^{11}	2.7×10^7	7.2×10^3
	10^{12}	4.2×10^7	3.0×10^3
	10^{13}	1.1×10^8	1.5×10^3
10^{17}	10^{10}	2.8×10^7	3.0×10^3
	10^{11}	7.7×10^7	2.4×10^3
	10^{12}	1.5×10^8	1.6×10^3
	10^{13}	7.8×10^8	1.5×10^3
Pulled 10^{17}	10^{13}	1.75×10^8	1.7×10^3

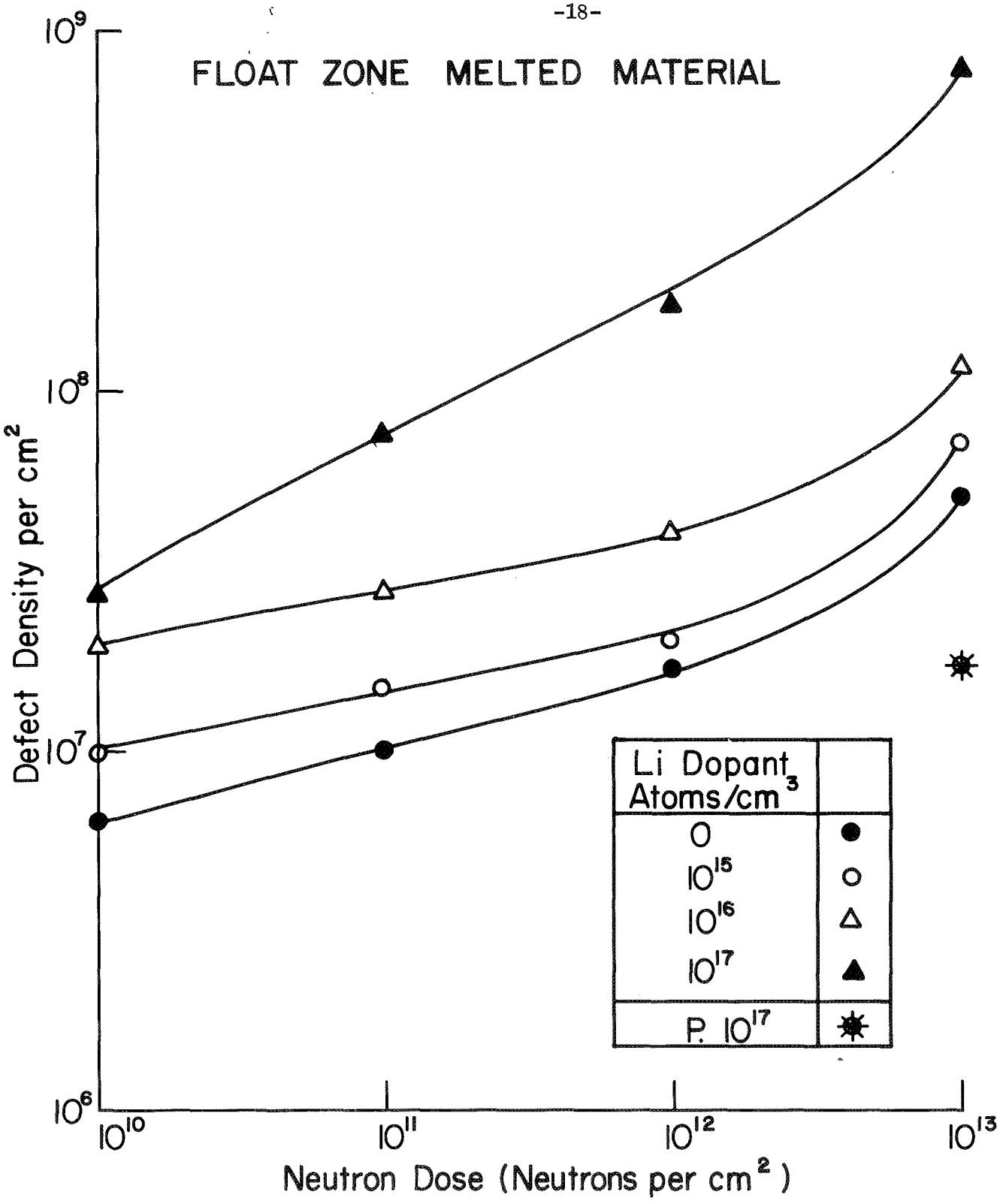

Figure 9. Average defect density as a function of irradiation dose and lithium doping.

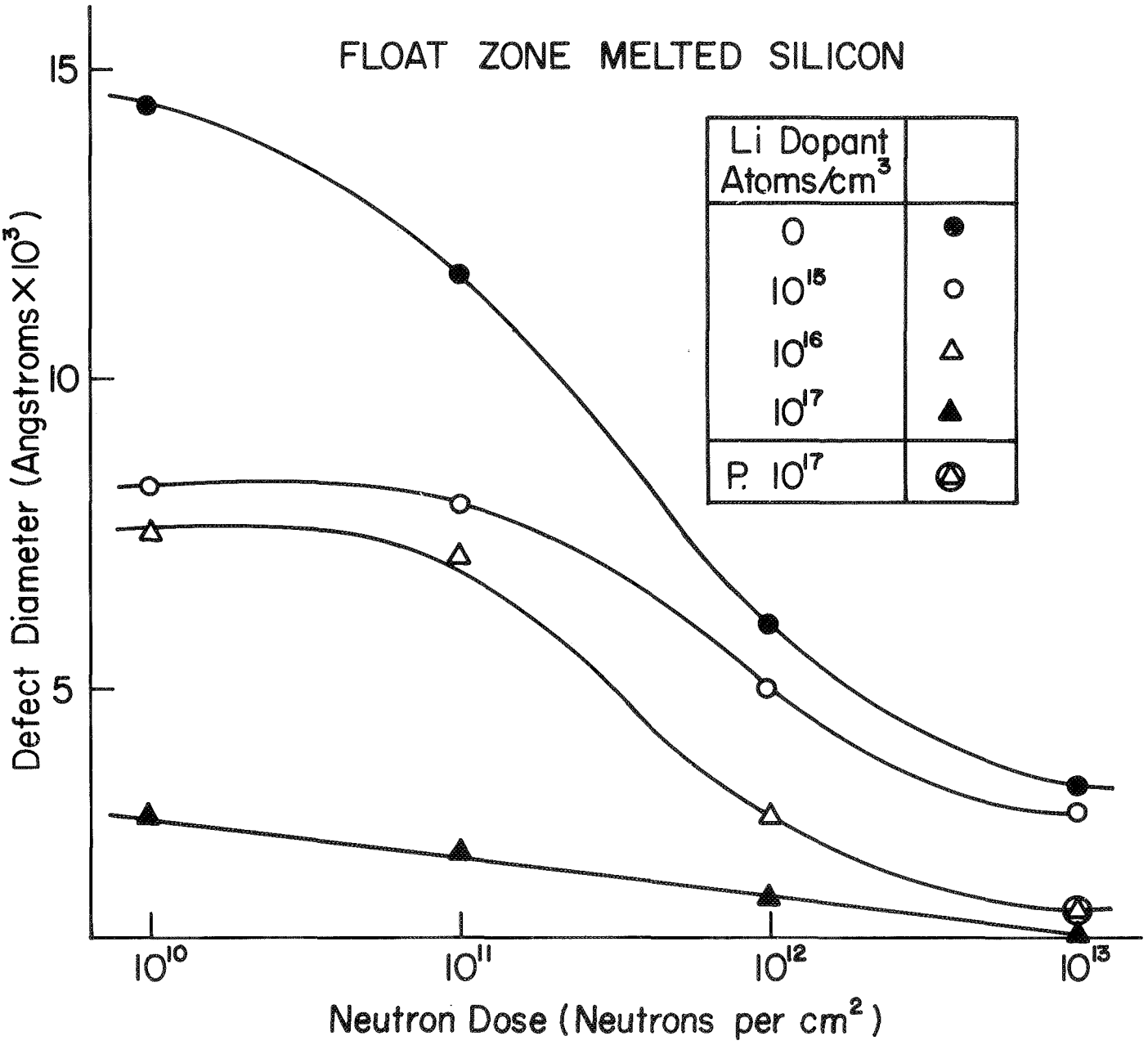

Figure 10. Average defect diameter as a function of neutron dose and lithium doping.

average crater density, for a given dose and doping level was found to be about 25%.

From Figure 9 it can be seen that the defect density increases with increasing irradiation dose, and furthermore, the defect density is higher in specimens which contain greater amounts of lithium. On the other hand, however, from Figure 10 it can be seen that the average defect diameter decreases with increasing dose and increasing lithium. Comparing Figures 9 and 10 it would seem that at a constant dose, there appears to be a balance between the defect density and the defect diameter. This tends to suggest that for a given dose the total defect volume is relatively constant. However, the presence of lithium provides more nucleation sites for the defect clusters to form, and as a result, the defect diameter is smaller.

Under comparable irradiation conditions (14 MeV neutrons at a dose of $10^{12}/cm^2$), the present results agree well with those obtained by Bertolotti et al (22) on pure silicon. According to the theoretical calculations of Bertolotti et al (21) the damage region in the silicon lattice should be of the order of about 500Å in diameter to give rise to a space-charge region of the order of 2000-2500 Å in diameter. With the exception of the present studies, direct observation by transmission electron microscopy has failed to reveal the presence of such large damage regions. However, the purity of the starting material may be of considerable importance here as well as the energy and dose of the irradiation. For example, Hemment and Gunnersen (15) were unable to observe any defects in neutron irradiated n-type silicon by transmission electron microscopy, however, their material was of very high resistivity ($\rho \simeq 1300\ \Omega$-cm), which probably indicates that it was very impure. Therefore, defects formed during irradiation would most likely become trapped by the impurities and would not form large clusters. More recently, Magee and Morriss (23) have studied neutron irradiated silicon by transmission electron microscopy and have observed defect clusters approximately 22 Å

in diameter. This result agrees well with the defect diameters observed by Pankratz, Sprague and Rudee (16). However, Magee and Morriss (23) also observed some larger defect clusters with diameters above 100 Å which they concluded were related to closely spaced individual clusters. It does not seem to be unreasonable, therefore, that with higher energy irradiation and with greater doses the defect clusters could become much greater than 100 Å in diameter and give rise to the space-charge phenomenon.

3.1.2 Annealing Experiments on Float Zone Material

Within the experimental error of the average defect density and diameter measurements it was found that no annealing occurred in the temperature range 300°K to 900°K, with the exception of those specimens which were undoped and which were irradiated at the two lowest doses, i.e. 10^{10} and 10^{11} neutrons/cm^2, respectively. Although these two batches showed no annealing at temperatures of 500°K and 700°K, there appeared to have been some annealing at 900°K. It was decided, therefore, to anneal some of the specimens at a higher temperature (1200°K). Time did not permit annealing all of the irradiated and doped samples to higher temperature, so a representative sample was chosen; namely, those samples containing no lithium irradiated at does of 10^{10} and 10^{13} neutrons/cm^2 and those samples containing 10^{17} lithium atoms/cm^3 irradiated at 10^{11} and 10^{13} neutrons/cm^2.

The results of these annealing experiments are presented in Table 2, and are shown graphically in Figures 11 and 12, respectively. It can be seen that those samples which had been irradiated at a high dose or those which contained the largest amounts of lithium suffered no annealing either by way of changes in the defect density or by way of changes in defect diameter. However, those which were undoped and irradiated at the lowest dose of 10^{10} neutrons/cm^2 showed considerable annealing at temperatures of 900°K and 1200°K. This is reflected in both an increase in the defect density and in a decrease in the defect diameter with an increase in the annealing temperature. It would appear from these results,

TABLE 2

Effect of Annealing Temperature on Defect Density and Defect Size

Temperature (°K)	Dose Φ (n/cm^3)	Lithium ($atoms/cm^3$)	Average Density ($\#/cm^2$)	Average Size (Å)
300	10^{10}	0	6.5×10^6	1.5×10^4
500			6.8×10^6	1.42×10^4
700			9.4×10^6	1.1×10^4
900			5.5×10^7	3.6×10^3
1200			9.2×10^7	3.2×10^3
300	10^{13}	0	5.4×10^7	3.5×10^3
500			4.9×10^7	3.4×10^3
700			5.0×10^7	3.6×10^3
900			$5.5. \times 10^7$	3.8×10^3
1200				
300	10^{11}	10^{17}	7.7×10^7	2.4×10^3
500			7.5×10^7	2.2×10^3
700			7.2×10^7	2.5×10^3
900				
1200			6.6×10^7	2.8×10^3
300	10^{13}	10^{17}	7.8×10^8	1.2×10^3
500			7.5×10^8	1.0×10^3
700			7.5×10^8	1.2×10^3
900			7.5×10^8	1.1×10^3
1200			5.2×10^8	1.8×10^3

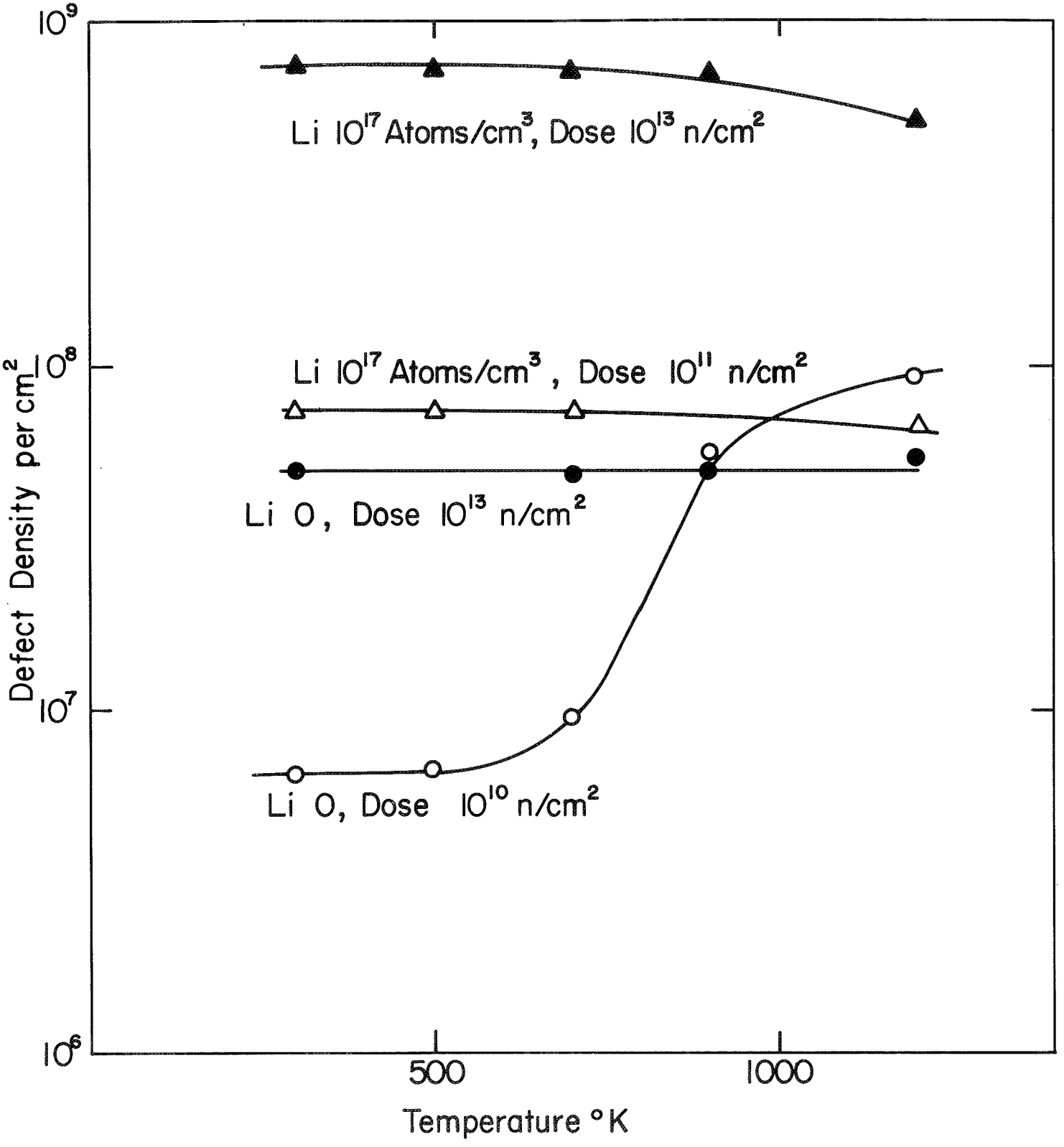

Figure 11. Effect of annealing on defect density.

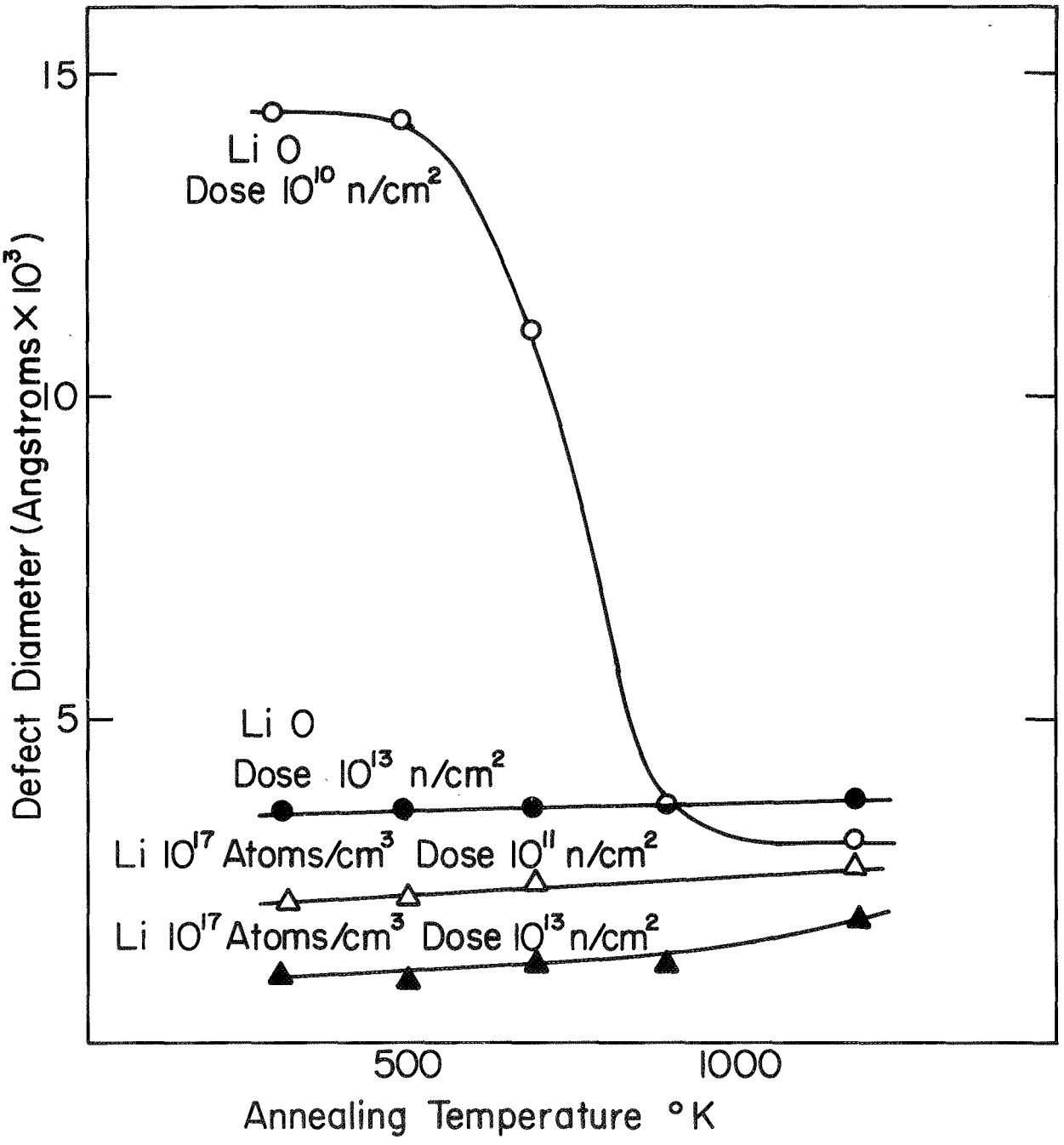

Figure 12. Effect of annealing on defect diameter.

therefore, that the defect structure which is formed during the irradiation at room temperature of either the undoped or doped material, at the highest doses,represents the most stable defect size. Upon annealing, the large defect clusters formed at the low doses in the undoped material seem to have a tendency to collapse to form small defects at a higher density.

The results of the annealing experiments carried out in the present work appear to be significantly different from those observed previously, from the recovery of electrical properties in neutron irradiated silicon, by Stein (24) and Passenheim and Naber (25). Stein (24) measured the neutron damage at 293°K by the degradation of the minority - carrier lifetime. On annealing the observed damage recovery to occur over a broad temperature range from 330°to 500°K. Passenheim and Naber (25), who carried out similar minority-carrier lifetime measurements on lithium doped silicon, found nearly complete recovery at about 380°K. However, it is not possible to correlate directly the present results with those of Stein and Passenheim and Naber for the following reasons. The annealing times for the present experiments were much shorter, 10 minutes as compared to 30 minutes to 1 hour; the neutron energies were higher in the present experiments, being 14 MeV as compared to about 1 MeV for reactor generated neutrons; and the neutron dose was considerably higher, 10^{10} to 10^{13} neutrons/cm ^{2} compared with 10^{10} maximum in the Stein and Passenheim and Naber experiments. In the present experiments a large decrease in the defect diameter and an increase in the defect density was observed; in the undoped material irradiated at the lowest dose of 10^{12} neutrons/cm^2, at a temperature of about 700°K. If the annealing time had been longer it is possible that this recovery could have been completed at a temperature closer to 500°K, and therefore the results would agree reasonably well with those observed by Stein (24).

It is not clear from the present results what role lithium plays in the nucleation and stabilization of the defects. At the high temperature used in the annealing experiments it is unlikely that the lithium would

remain in the bulk. However, it is possible that at the irradiation temperature the neutron irradiation produced defects are trapped at precipitated metallic lithium and form stable clusters. The subsequent annealing of the cluster, once it has reached a stable configuration or critical size, could be independent of the presence of the lithium. Hence, the mobility of the lithium at the higher annealing temperature would not necessarily influence the annealing kinetics of the defect cluster.

3.2 The Crucible Pulled Solar Cell Material

3.2.1 Neutron Irradiation and the Effect of Lithium Doping

A thin film electron transmission photomicrograph of the undoped pulled solar cell material is shown in Figure 13. The structure contains many dark spots which appear to be precipitates, possibly some form of oxide. Figure 14(a) shows a selected area diffraction pattern taken of an area such as that shown in Figure 13. The diffraction pattern shows diffraction spots which one would expect from a (100) crystal slice. However, in the original photographic plate a number of additional but weaker spots could be resolved, which could not be indexed with that of the matrix. It seems highly probable that these additional diffraction spots are associated with the precipitates which were observed in the transmission picture. However, it was not possible to accurately index these spots and further identification of their origin is impossible using the present technique. An interpretation of the diffraction pattern, showing the positions of the unidentified diffraction spots, is shown in Figure 14(b). A similar pattern was obtained for the doped samples; however, in this case, unlike the float zone refined material, there was no direct indication that lithium was associated with the precipitates observed in the undoped material. The additional spots in this instance could not be indexed as belonging to the body-centered cubic structure.

Figure 15 shows a photomicrograph of a surface replica taken from a doped, but unirradiated, pulled specimen. Although circular type objects can be observed here, they are not typical of the craters produced

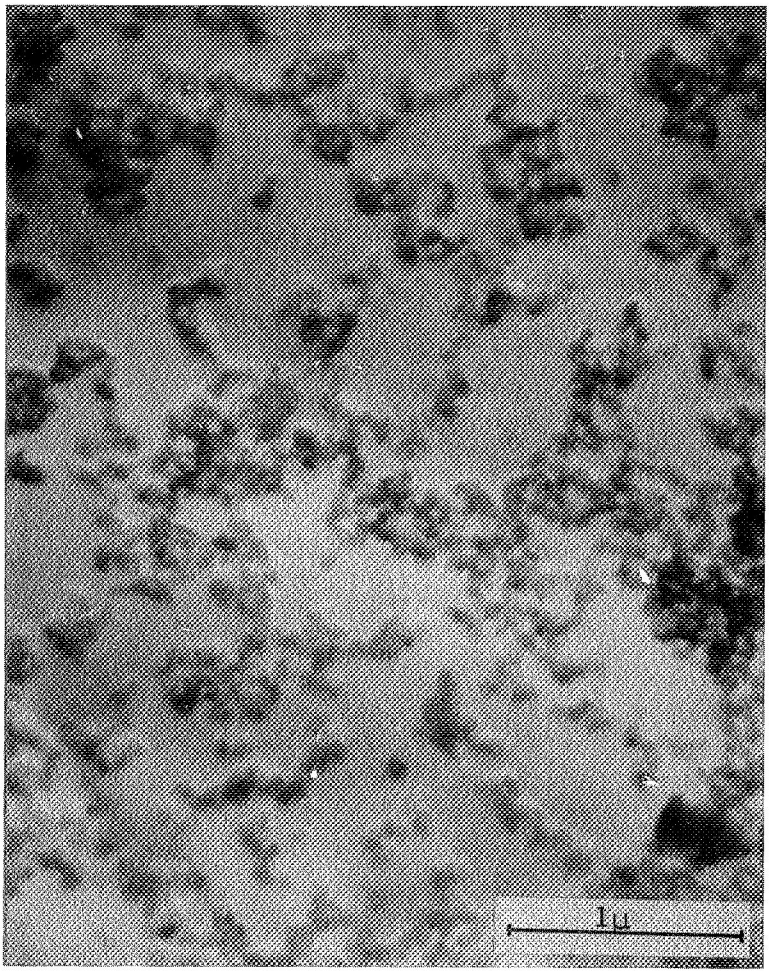

Figure 13. Transmission electron photomicrograph of the as-received crucible pulled solar cell material.

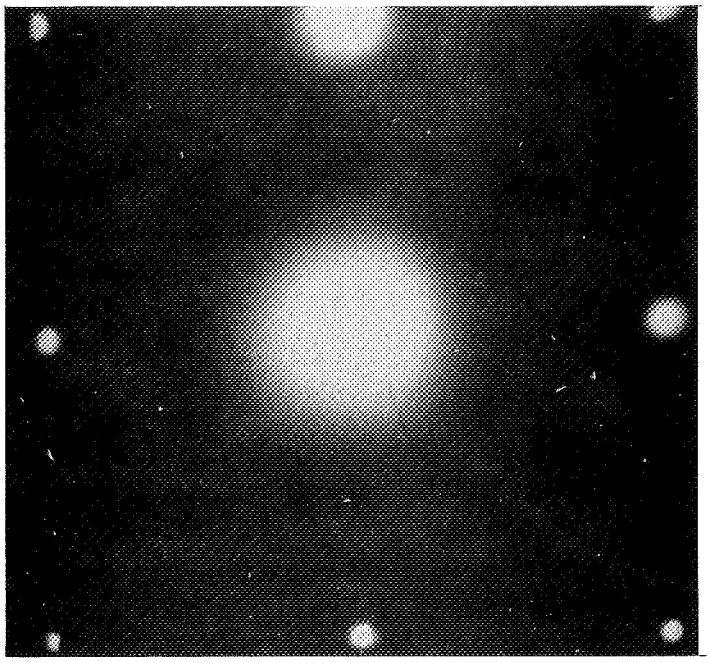

Figure 14(a). Selected area diffraction pattern of the as-received crucible pulled material.

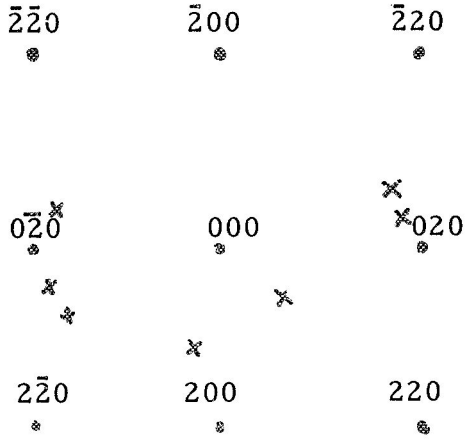

Figure 14(b) Interpretation of selected area diffraction pattern shown in Figure 14(a).

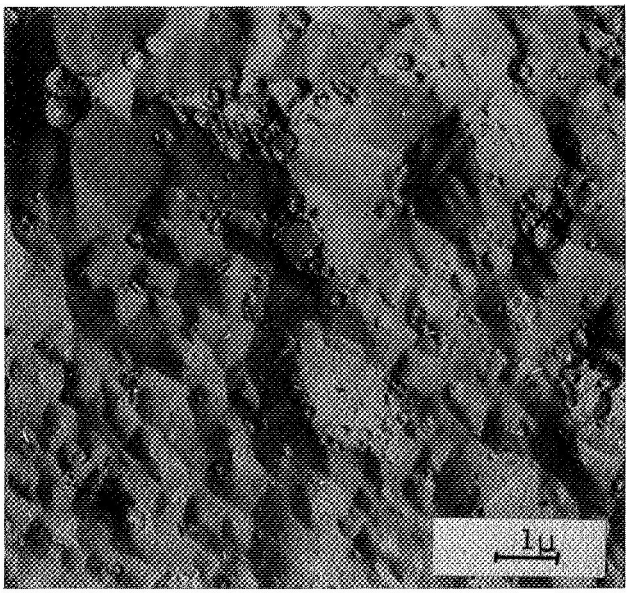

Figure 15. Surface replica of the unirradiated crucible pulled material.

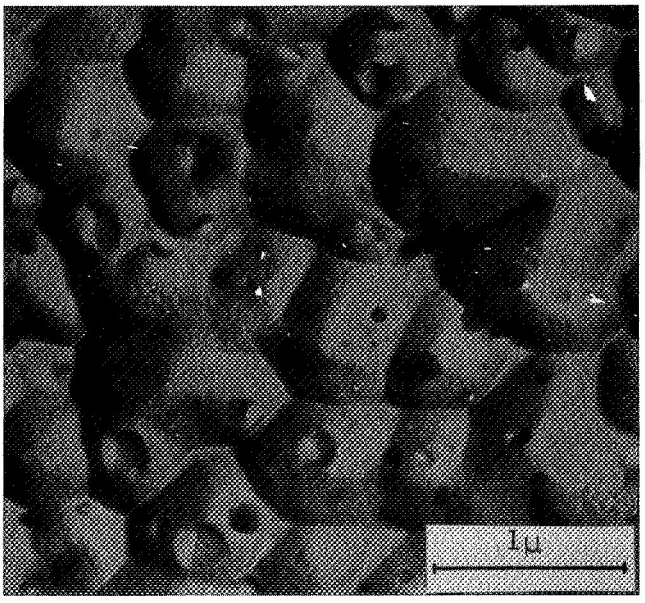

Figure 16. Surface replica of the doped (10^{17} lithium atoms/cm^3) and irradiated (10^{13} n/cm^2) crucible pulled material.

by irradiation damage as were observed in the float zone material. This structure appears to be more representative of the type of damage which is produced by the evolution of gas bubbles during etching of the surface. It is possible that vigorous etching occurred in the region of the precipitates revealed in the transmission electron photomicrographs.

The surface attack shown in Figure 15 was observed in all the samples examined with the exception of those samples containing 10^{17} lithium atoms/cm^3, which were heavily irradiated. In this case, as can be seen in Figure 16, the surface replica shows a structure which contains crater like defects the same as those observed in the float zone irradiated material.

It is not clear at the present time why the crater type defects are not visible at the lower doping levels in the irradiated condition. It is probable, however, that in this material dissolved oxygen acts as a very efficient trapping center for irradiation induced defects, thus preventing large defect cluster, such as those revealed by the craters, from forming. At high lithium concentrations it is possible that most of the oxygen combines with lithium and is precipitated out of solution as lithium oxide, therefore reducing its trapping efficiency. Thus it requires a combination of a high lithium doping level to remove the oxygen traps and a high irradiation dose to provide sufficient numbers of defects to create conditions which are suitable for the formation of the large crater producing defect clusters.

The average defect density for the lithium doped (10^{17} atoms/cm^3) and irradiated (10^{13} n/cm^2) sample was 1.75×10^8 defects/cm^2 and the average size was 1.65×10^3 Å. These values are plotted on Figures 9 and 10 respectively, for comparison with the float zone material.

It can be seen that the crater defect density in the pulled material is considerably less than that which was observed in the float zone material. However, the average defect diameter appears to be about

the same. The low defect density and small defect size is probably the reason why the crater defects could not be resolved at the lower irradiation doses even in the heavily doped material.

3.2.2 Annealing Experiments on Crucible Pulled Material

Due to the experimental difficulties mentioned in the previous section associated with revealing the defects, the annealing experiments were confined to the sample doped with 10^{17} lithium atoms/cm^3 and irradiated with 10^{13} neutrons/cm^2. It was observed that over the temperature range 300° to 900°K, no change in defect density or size could be detected. However, upon annealing to 1200°K, it was found that the defect density had dropped to zero.

3.3 Effect of Crystal Orientation

In the present series of experiments it was only possible to obtain crystals which were sliced (110) for the float zone refined material and (100) for the pulled material. However, in the case of the float zone material, it was decided to attempt to measure the effect of orientation on structural damage produced simply by orienting the slice at different angles to the irradiating source. It was found, however, that the neutron beam produced by the Cockroft-Walton generator cannot be sufficiently well directed so as to be selective with one particular direction. The main problem appeared to be associated with the fact that a large amount of radiation is scattered indiscriminately from the walls of the irradiation cave. Therefore, under the present experimental conditions, no effect of orientation was observed.

4. SUMMARY AND CONCLUSIONS

1. There was found to be some evidence that, at the lithium doping levels considered in the present experiments, some metallic lithium exists in the lattice in the form of a fine precipitate.

2. Crater like defects; revealed by surface replications, were observed in the irradiated specimens. These were found to range in size from about 1500 Å to 15,000 Å depending upon the irradiation dose and lithium dopant content. With the exception of those samples irradiated at the lowest dose, the craters were found to be similar in size and appearance to those observed by Bertolotti (19-22) and were found to have characteristics similar to those predicted by the theory of Gossick (7); i.e., the craters appear to be associated with the space charge region which surrounds a cluster of irradiation induced defects which are most probably lattice defects.

3. The crater defect density was found to increase and increasing lithium doping level, from about 6.5×10^6 defects/cm^2 for no lithium and a dose of 10^{10} neutrons/cm^2 to 7.8×10^8 defects/cm^2 for 10^{17} lithium atoms/cm^3 and a dose of 10^{13} neutrons/cm^2.

4. The crater diameter was found to decrease with increasing irradiation dose and increasing lithium dopant, from about 1500 Å in the undoped material at a dose of 10^{10} neutrons/cm^2 to about 1500 Å for 10^{17} lithium atoms/cm^3 and a dose of 10^{13} neutrons/cm^2.

5. The total defect volume, for a constant irradiation dose appears to be constant. The presence of lithium atoms or precipitates causes an increase in the defect density and a reduction in the average defect size.

6. No annealing of the crater defect structures was observed in the temperature range 300° to 900°K, with the exception of the undoped samples irradiated at doses of 10^{10} and 10^{11} neutrons/cm^2. In these cases it was found that the defect diameter decreased rapidly, and at the same time there was a significant increase in defect density. It may be concluded that lithium acts as a trapping center, and hence, presents sites at which nucleation of the defect cluster can occur.

7. In the pulled material some form of precipitate, most probably an oxide, was observed in the undoped and doped specimens. This could not be identified explicitly.

8. In the pulled material crater-like defects could only be resolved in the most heavily doped (10^{17} lithium atom/cm^3) and irradiated (10^{13} n/cm^2) specimens. In this case, the defect density was found to be considerably less than that which was observed in the float zone material, while the average defect diameter was about the same. It was concluded that oxygen in the pulled material probably is a very efficient trap and that it may react with the lithium forming an oxide precipitate. In this condition it is less efficient as a trap and the crater producing defect clusters can then form, providing the irradiation dose is sufficiently high.

9. No effect of crystal orientation was found under the present experimental conditions.

5. NEW TECHNOLOGY

No new technology is currently being developed or employed in the present program.

6. PUBLICATIONS

"The Observation of Structural Damage Produced by Neutron Irradiation in Lithium Doped Silicon Solar Cells by Transmission Electron Microscopy", Submitted to Journal of Applied Physics, 1970.

REFERENCES

1. F. Seitz, Discussions Faraday Soc. 5, 271, (1949).
2. F. Seitz and J. S. Koehler in Solid State Physics, edited by F. Seitz and D. Turnbull (Academic Press, Inc., New York, 1956), Vol. 2.
3. S. Siegel, Phys. Rev. 75, 1823, (1949).
4. D.S. Billington, Nucleonics 14, 54, (1956).
5. H. Brooks, Am. Rev. Nuclear Sci. 6, 215, (1956).
6. H.M. James and K. Lark-Horovitz, Z. Physick Chem. (Leipzig), 198, 107, (1951).
7. B. R. Gossick, J. Appl. Phys. 30, 1214, (1959).
8. J. H. Crawford and J. W. Cleland, J. Appl. Phys., 30, 1204, (1959).
9. W. H. Closser, J. Appl. Phys., 31, 1693, (1960).
10. H. J. Stein, J. Appl. Phys., 31, 1309, (1966).
11. H. J. Stein, Phys. Rev. 163, 801, (1967).
12. H. J. Stein, J. Appl. Phys., 39, 5283, (1968).
13. F. E. Fujita and U. Gonser, J. Phys. Soc. Japan, 13, 1968, (1958).
14. J. R. Parsons. R.W. Balluffi and J. S. Koehler, Appl. Phys. Letters, 1, 57, (1962).
15. P. L. F. Hemment and E. M. Gunnersen, J. Appl. Phys., 37, 2912, (1966).
16. J. M. Pankratz, J. A. Sprague and M. L. Rudee, J. Appl. Phys., 39, 101, (1968).
17. R. Chang, J. Appl. Phys., 28, 868, (1957).
18. T. S. Noggle and D. J. Stiegler, J. Appl. Phys., 30, 1279, (1959).
19. M. Bertolotti, et al., Neuoro Cimento, 29, 1200, (1963).
20. M. Bertolotti, et al., J. Appl. Phys., 36, 3506, (1965).
21. M. Bertolotti, et al., J. Appl. Phys., 38, 2645, (1967)
22. M. Bertolotti, "Radiation Effects in Semiconductors", Plenum Press, 311, (1968).
23. T. L. Magee and R. H. Morriss, Bulletin., Am. Phys. Soc., 15, 1367, (1970).

24. H. J. Stein, J. Appl. Phys., 37, 3382, (1966).

25. B. C. Passenheim and J. A. Naber, 'Radiation Effects', 2, 229, (1970).

For other information address:

Office of Research and Engineering Services
Publication Services
College of Engineering
University of Kentucky
Lexington, Kentucky 40506